J Appl Electrochem (2012) 42:399–407
DOI 10.1007/s10800-012-0413-5

ORIGINAL PAPER

Enhanced performance of hybrid power source under low temperature

Guoyu Zhang · Xiaowei Zhao · Bin Wang · Feng Tian · Jiaxi Qiang · Lin Yang

Received: 27 February 2012 / Accepted: 9 April 2012 / Published online: 22 April 2012

Abstract The performance of a battery–electrical double layer capacitor (EDLC) hybrid power source at low ambient temperature has been experimentally analyzed. EDLC can enhance the performance of lead-acid battery as it acts as a buffer during charging and discharging, and plays more significant role at low temperature than room temperature. The behaviors of current and voltage of both battery and EDLC have been detailed studied, and described by a mathematical model. With EDLC assistance, the battery can maintain longer discharge duration at −25 and −10 °C, compared with the battery alone. Adding an EDLC in parallel with the battery exhibits a considerable capacity increase compared to battery standalone in continuous discharge processes: from 13.6 to 36.5 %, corresponding to 25 to 200 A. These improvements of capacity become even more significant at low temperature. The increases in available capacity of different pulse duty, amounted to 72, 58, and 4 % at 0.1, 0.5, and 0.9 duty cycle values, compared to the capacity measured at constant current rate, respectively (calculated by 50 A discharge).

Keywords Lead-acid battery · Electric double layer capacitor · Low temperature · Hybrid power source

1 Introduction

The rapid development of electric vehicles (EVs) or hybrid electric vehicles (HEVs) requires the energy source to provide more efficient and sustainable propulsion. The energy sources should meet several operational requirements such as sufficient energy/power capabilities, sufficient life time, and low cost. Unfortunately, there is no single available energy source (battery or supercapacitor) on the market that satisfies all these qualifications. Designers usually have to confront trade-offs between the energy density and power density or between the performance and operation life.

Batteries and electric double layer capacitors (EDLCs) are electrochemical energy storage devices with different mechanisms for the energy storage. While EDLCs ideally store the electrostatic energy in the electric field of the electrochemical double layers [1], batteries work as the bulk of the respective electrode material charging energy via redox reactions. Consequently, the specific energy stored in an EDLC is relatively low due to limitations in the accessible specific surface area of the electrode, while the specific power of EDLC is rather large since the lower internal resistance and it operates only involve absorption and desorption. On the other hand, the battery has much higher energy density owing to the continuous chemical reactions that take place on the electrodes, while it has relatively smaller power density because the charge/discharge processes are mainly limited by the reaction rate. Therefore, modern EV/HEV is usually equipped more than one energy source to provide desired performance [2–4]. A common structure of the EV's energy storage system is to combine the battery pack and the EDLC pack with or without a bi-directional DC/DC convertor. This topology is widely used since it can be easily obtained by the single power sources structure with few modifications. In spite of that, the isolated packs of batteries and supercapacitors in this configuration still have some drawbacks as they were separately used. For instance, the EDLC cannot absorb the transient current for

G. Zhang · X. Zhao · B. Wang · F. Tian · J. Qiang · L. Yang (✉)
School of Mechanical Engineering, Shanghai Jiaotong University, 800 Dongchuan Road, Shanghai, China
e-mail: powervr@163.com

individual battery cell and this may accelerate the degradation of some battery cells with lower terminal voltage. An improved structure of hybrid power source (HPS) is therefore brought out to make up for the shortcomings. In the work of Bentley et al. [2–4], an integrated cell combined with a VRLA cell and supercapacitor cell in series was proposed. The testing drive cycle included sections of urban stop–start driving, aggressive driving on the hill circuit and motorway driving with high speed. Those results have shown the cell current was reduced and the EDLC has sunk the majority of transient current. However, Holland et al. [5] tested a Li-ion cell coupled with EDLC under a simple pulsed current load which provided only marginal increase in available capacity. They indicated that the directly parallel connected battery/EDLC cells are not likely to be practical for the EV/HEV applications, especially when evaluating the hybrid system on a mass basis.

Although the issue of using the hybrid cells as the peak power source (PPS) of EV/HEV is still controversial, it seems feasible to adopt this structure to the traditional vehicle cranking system, particularly for a vehicle operating in cold countries. Because in such application, the battery undergoes a high rate pulse discharge every time the engine starts. It was well documented in the paper of Smith [6], high power discharge and charge pulses may reduce overall VRLA cell runtime, and overall battery health, mainly by the following reasons:

(a) Physical degradation of the cell structure. This gives rise to considerably shorter cell lifetime, due to increased grid corrosion, and increased gassing with the cell, leading to separator drying out, and eventual cell failure.
(b) Higher currents lead to reduced available capacity. This is caused by the isolation of active material due to the blocked pores by sulphate deposition during the high rate discharge. Also the reaction rate may outstrip the diffusion rate, causing a depletion of ions at the reaction surface [7, 8].

Besides these, high current pulses will cause dramatically cell voltage drop in low temperature environment, since the internal resistance of the battery is much greater than the value of room temperature. These low-voltage pulses may trip low-voltage limit detection system to protect the battery in closely managed battery pack. In some extreme cold area, the engine cannot be cranked because the battery performance is too bad to meet the current demand, even though the SOC level is relatively high. Consequently, how the EDLC can improve the power and life performance of the lead-acid battery under low temperature is worth to research.

This paper focuses on the low temperature improvement gained by this topology in terms of their energy and power capabilities. Pulse discharge tests under various ambient temperatures are conducted in this paper to figure out the different performances and characteristics of the HPS compared to the single battery cell. A Urban Dynamometer Driving Schedule (UDDS) drive cycle laboratory test also has been proposed to evaluate the performance of HPS as the PPS in EV/HEV.

2 Experiments

2.1 Experimental setup

The layout of the experimental system is presented in Fig. 1. A 55 A h (nominal capacity) vehicular lead-acid battery (model GM9022317) is parallel connected with an EDLC (model MDLE15R0V383FB0). Main parameters of the battery cell and EDLC are listed in Table 1. To evaluate how well the HPS performs, a battery of the same type is used as a reference for the comparison. The hybrid system is recharged before each test by Digatron BTS-600 battery test system. The power supply's output channel is rated at 0–60 V DC at a maximum current output of ±400 A. Currents are measured by Hall effect sensors that connected to a data acquisition terminal. This acquisition system is accomplished using LabVIEW software manufactured by the National Instruments Corporation.

2.2 Pulse discharge test

To make the results more comparable, before starting each test, the power supply charges the HPS at a constant current of 30 A until the terminal voltage reaches 16 V, and it switches to a constant voltage of 16 V for 4 h. The pulse discharge experiments under various ambient temperatures are conducted so as to study the performance differences between the HPS and battery standalone, and the discharge tests are listed in Table 2. There is an hour's interval

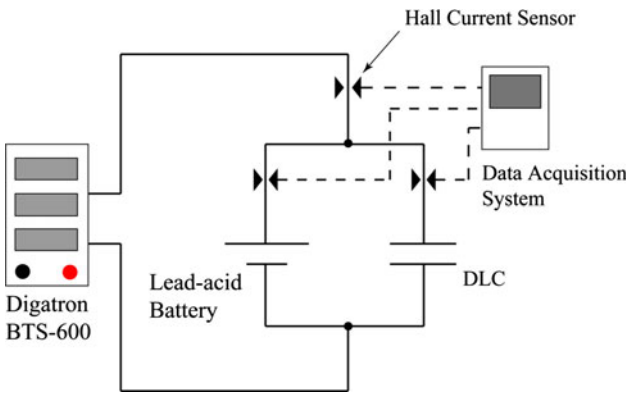

Fig. 1 Experimental layout of hybrid power source

Table 1 Capacity, internal resistance for the battery cell and EDLC module

Element	Nominal capacity (A h)	Internal resistance (mΩ)
Battery GM9022317	55	5
EDLC MDLE15R0V383FB0	0.39 (at 15 V) (282 F)	2.3

Table 2 The pulse discharge profile

	25 °C	−10 °C	−25 °C
300 A	●	●	●
200 A	●	●	●
100 A	●	●	●

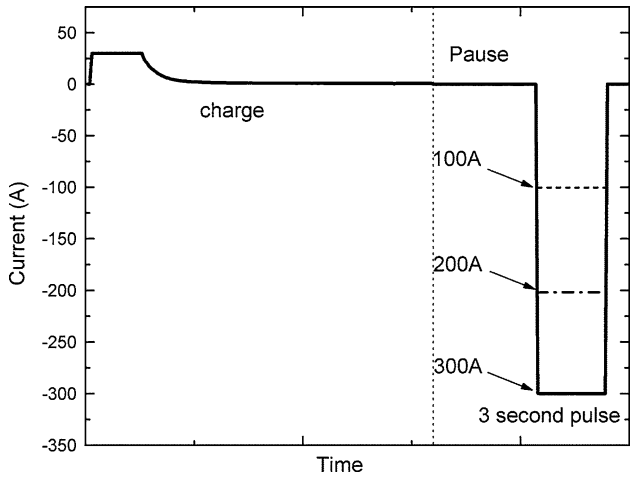

Fig. 2 The typical pulse discharge procedure of the power source and the battery

between the charge and discharge stages, giving enough time to make the battery voltage dropping to a steady level. To protect the battery, all tests will be terminated when system voltage drops below 10 V. Both the HPS system and the battery had an 8-h cold soak at constant temperature (for the tests under −25 and −10 °C) before the tests, respectively. The pulse discharge experiments are planned to perform at 100 % battery SOC to avoid possible interruptions by the unnecessary voltage drop when high rate pulse applied on the battery, especially in the low temperature tests. The standard procedure for pulse discharge tests is shown in Fig. 2. The *X*-axis comes in a uniformed time scale, because it displays more well in two time scales for two different stages. The charge and pause procedures come in a time scale of 1 min, while 0.5-s interval for pulse discharge.

2.3 Dynamic endurance test

One common parameter which is closely related to the state of health (SoH) is the actual battery capacity, which varies in function of the state of charge, temperature, and Peukert constant. From this point of view, Omar et al. [9] studied the capacity of the battery without/with EDLC's versus number of cycle. Their results have illustrated that the configuration with EDLC at the beginning of the test has a SoH of around 86 % in comparison with 70 % in the case without EDLC's, and the battery–EDLC combination operates from cycle 1–50 in a wider SoH (86–20 %) window instead of 70–0 % without EDLC. However, their experiments were performed merely at room temperature and with fixed pulse duty cycle (60-s 50 % duty cycle discharge pulse consisting of two different rates). To further study how an EDLC assisted battery improves the performance in pulse discharge processes of different duration and duty cycle, a set of tests are performed. The HPS are subject to the same current profile (as shown in Fig. 3) under 25 and −25 °C, respectively. To make the results more comparable, all the pulses corresponding to specific current rate and duty cycle have the same time duration of 10 s. The tests are listed in Table 3. Each test is consisting of a set of sub-cycles (black regions in Fig. 3) with:

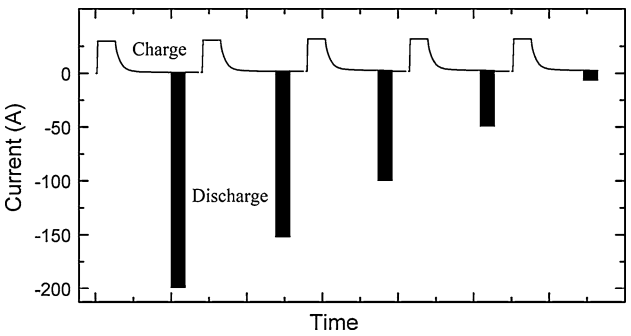

Fig. 3 Pulse discharge test profile

Table 3 Pulse discharge tests according to different current rates and duty cycles

Current (A)	Duty cycle (s)		
	10 %	50 %	90 %
25	10	10	10
50	10	10	10
100	10	10	10
150	10	10	10
200	10	10	10

Table 4 Main parameters of the vehicle model

Parameter	Value
Vehicle mass (kg)	989 (curb weight)
C_g (m)	0.5 (estimated for 1995 Saturn SL)
Frontal area (m^2)	2.0
C_D	0.335
Wheelbase (m)	2.6

- A current pulse with fixed rate (2, 5, 50, 100, 150, and 200 A during 1 s/5 s/9 s);
- No current for pause period (9 s/5 s/1 s).

This discharge cycle will be looped until the cut-off voltage of 10 V is reached. Further the battery will get a 30-min break before to start with the charging. The charge process in this test is according to the procedure mentioned in Sect. 2.2. The time axis in Fig. 3 is only a schematic diagram.

2.4 Drive cycle test

Using a mathematical vehicle model (the main parameters are listed in Table 4) implemented by ADVISOR which is widely used for performance simulation and analysis of EV/HEV, the input drive cycle (UDDS) data can be converted to desired power map. After that, the data should be scaling down to match a single HPS unit. The number of HPS unit used in the vehicle is 32 (384 V/12 V). The power that one HPS unit will share is therefore 1/32 of the total power demand. This rescaled power data is then sent to the test equipment as an input profile.

3 Results and discussion

3.1 Characteristic of current and voltage

The results of 300 A pulse discharge tests performed under −25, −10, and 25 °C are shown in Fig. 4, 5, and 6, respectively. They depict the contributions of the EDLC in the HPS under different temperatures. Figure 4 illustrates as an example of the current distribution between the two components at −25 °C. Under such low ambient temperature, the internal resistances (R_{int} or ESR) of both the battery and the EDLC will dramatically increase. The ions movement will be slowed down due to the high viscosity of the electrolyte at low temperature. Lower speed means larger conduction resistance. Thus, the R_{int} increases when temperature drops. According to the manufacturer's datasheet, the R_{int} (called DCIR in the datasheet) of the EDLC at −25 °C is four times larger than the nominal value measured at 20 °C. On the other hand, the battery performs

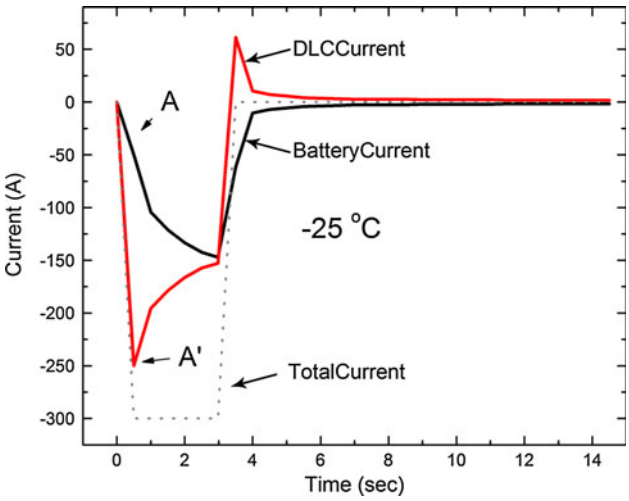

Fig. 4 The current distribution between battery and EDLC in HPS under 300 A pulse discharge (−25 °C)

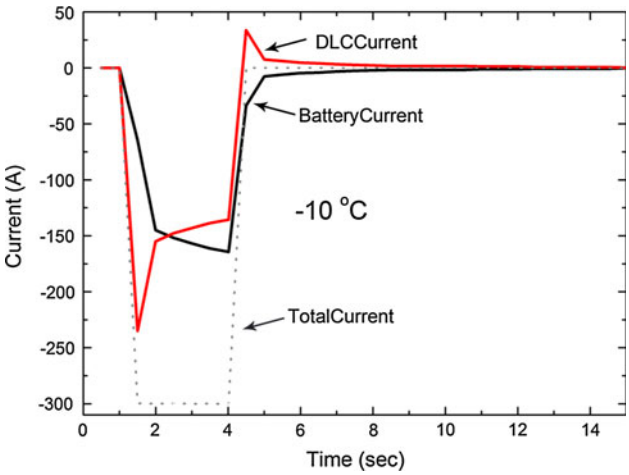

Fig. 5 The current distribution between battery and EDLC under 300 A pulse discharge (−10 °C)

even worse at such low temperature. Besides ions velocity, low temperature will also slow down the chemical reaction in the battery, which does not exist in the EDLC. This temperature dependent relation has been described by the Arrhenius Law,

$$k = A \exp\left(-\frac{E_a}{RT}\right), \quad (1)$$

where k is reaction rate, E_a is apparent activation energy, R is the gas constant (8.31 J mol^{-1} K^{-1} in SI system), and T is absolute temperature. The overall increase of inner resistance of the battery is therefore determined by the sum of the two effects. Figures 5 and 6 also show the similar distribution behaviors. The currents differences become smaller as temperature increases. Noticeably, at room

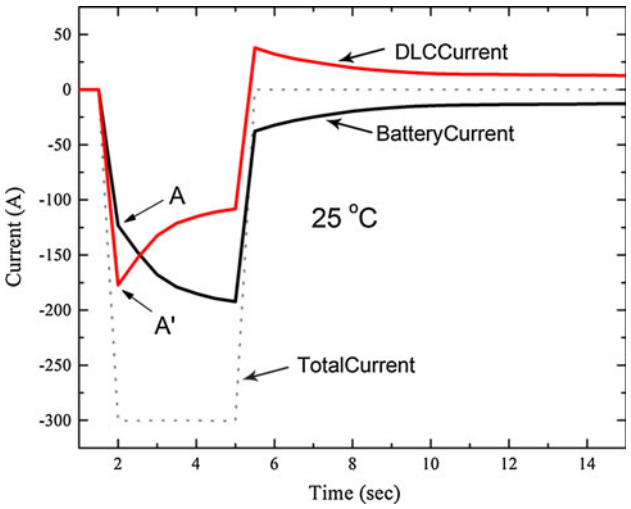

Fig. 6 The current distribution between battery and EDLC under 300 A pulse discharge (25 °C)

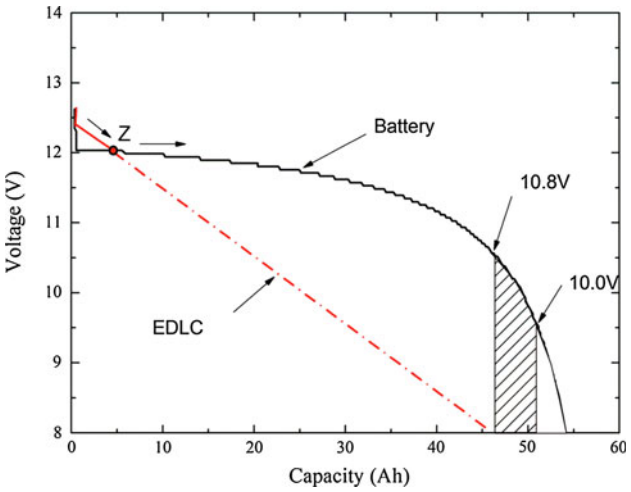

Fig. 7 A schematic diagram of the voltage variation of EDLC and lead-acid battery during discharge

temperature (shown in Fig. 6), the battery current proportion is over 50 % in more than 2/3 pulse time, since the difference of R_{int} between the EDLC and the battery becomes smaller compared to that at −25 °C.

From the results above, it can be observed that the capacitor takes a certain part of the total current demand during the pulse discharge stage, especially at the beginning (almost 90 % of total current in Fig. 4). One can simply ascribe this distribution pattern to the differences of inner resistance between the two components [8, 10]. However, the literatures were deficient in the explanation of the falling of EDLC current (or the rebound of battery current) after the pulse begins. Actually, different resistances of the two components only determine the transient current distribution at the beginning. Figure 7 is a sketch map that briefly explains the reason why the EDLC current falls after the pulse begins. Generally, EDLC capacity is linearly correlated with its terminal voltage (as the EDLC line shown in Fig. 7), and the battery has a more flat voltage window. At the first moment, the voltage of the EDLC is slightly higher than the battery's, due to the smaller internal resistance, thus it can share a certain portion of total current according to their ESR ratio. As time goes, the EDLC voltage falls with the loss of electric charges. On the other hand, its voltage has to be equal to the battery's terminal voltage because they are parallel connected with each other. From the Z-point in Fig. 7, the EDLC voltage will follow the battery voltage line and it has no charge to release. Consequently, the EDLC current has to fall.

To further study this phenomenon, an equivalent electric circuit model is established as Fig. 8. According to this model, Kirchoff's equations are listed as follows:

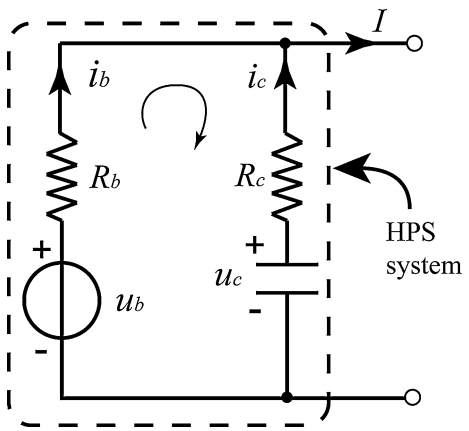

Fig. 8 Equivalent circuit for the hybrid power source (HPS)

$$i_{\text{b}} + i_{\text{c}} = I, \tag{2}$$

$$u_{\text{b}} - i_{\text{b}} \cdot R_{\text{b}} = u_{\text{c}} - i_{\text{c}} \cdot R_{\text{c}}, \tag{3}$$

where u_{b}, i_{b} represent the battery voltage and current, while u_{c}, i_{c} is the EDLC voltage and current, respectively. Therefore,

$$i_{\text{c}} = \frac{R_{\text{b}}}{R_{\text{b}} + R_{\text{c}}} \cdot I \cdot \exp\left[-\frac{t}{(R_{\text{b}} + R_{\text{c}})C}\right]. \tag{4}$$

Equations 2–4 are based on the following assumptions:

- The battery can be modeled as an ideal voltage source with internal resistance R_{batt}, due to the battery has a more flat and wide discharge platform compared to the EDLC, and the capacity loss of the battery during the pulse can be neglected (the electric charge released in a 3-s 300 A pulse is 0.25 A h, which takes only 0.45 % of the overall capacity of the 55 A h lead-acid battery);

- The EDLC voltage u_c is equal to the battery OCV u_b when $t = 0$;
- The total current demand I is constant with time which is in agreement with the experiments.

From Eq. 4, it can be seen that the EDLC branch current is determined by the ratio $R_b/(R_b + R_c)$ only at the beginning ($t = 0$) of the discharge pulse. After that, it decreases in the law of negative power exponent, and the time constant $\tau = (R_b + R_c)C$ is correlated with the *ESR* of the two components and the EDLC's capacity, respectively. This result is compatible with the experiments (Figs. 4, 5, 6). From −25 to 25 °C, the EDLC current varies more and more exponentially since τ decreases with the internal resistances of both battery and the EDLC. Take the current curves shown in Fig. 6 at 25 °C for example, the calculated value of EDLC current at the pulse beginning is given by $R_b \cdot I/(R_b + R_c)$, namely 199 A (using typical values in the data sheets: $R_b = 5\,\text{m}\Omega$, $R_c = 2.3\,\text{m}\Omega$), and the measured EDLC value at point A′ in Fig. 4 is 175 A, which is close to the predicted value. The difference between them may arise from the recording interval (0.5 s) of the data logger is not small enough to describe the system's transient behavior which occurred within the first few milliseconds. The experimental value of $\tau = 1.98$ can be determined by the nonlinear fitting method, which fits very well with the calculated value 2.03.

The current shared by the EDLC in the first 0.5 s of the pulses with respect to different current rates and different temperatures are calculated and summarized in Fig. 9. It is indicated that the EDLC could improve the poor performance of a solo battery in the low temperature and high rate discharge processes. Figures 10 and 11 illustrate the voltage behaviors of the HPS in the 300 A discharge pulse at −25 and −10 °C, respectively. Both the battery and HPS are not capable to sustain a 3-s discharge pulse due to the terminal voltage drops below 10 V, as shown in Fig. 10. But HPS can hold 2.5-s pulse duration, which is about 3 times longer than the solo battery. Battery voltage drops sharply when the current applied to it, and the discharge process stopped at Time = 0.9 s, namely 700 ms after the pulse beginning. In the −10 °C case (Fig. 11), although both of them could finish the entire test, the HPS still have a smaller voltage drop compared with the battery alone. As one can see in those tests, the HPS with EDLC assistance can set off the disadvantage of low voltage and enhance the performance of lead-acid battery, especially under extreme conditions.

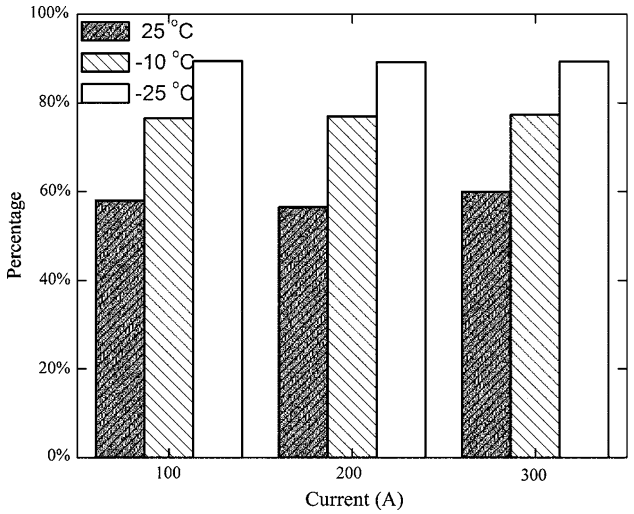

Fig. 9 Comparison diagram of current ratio of EDLC and battery at the first 0.5 s

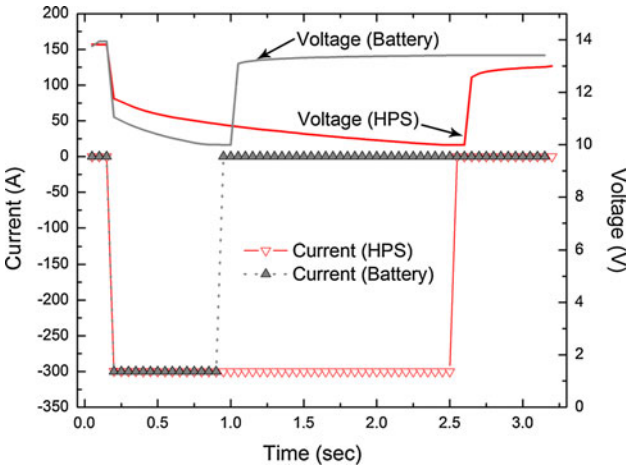

Fig. 10 The comparison diagram of discharge pulse duration and the terminal voltage drop between HPS and the battery (−25 °C)

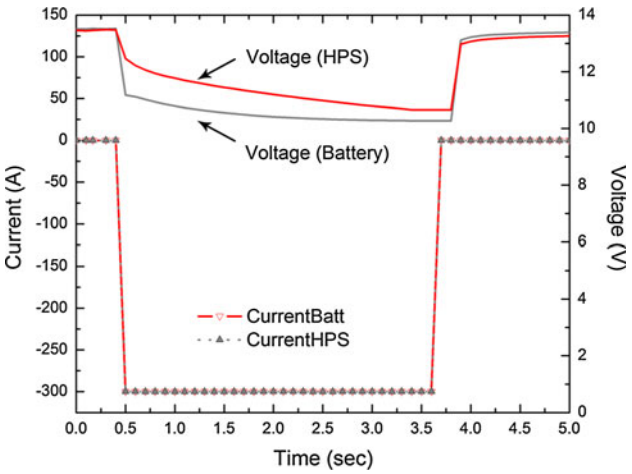

Fig. 11 The comparison diagram of discharge pulse duration and the terminal voltage drop between HPS and the battery (−10 °C)

Table 5 Peukert numbers and capacities of battery and HPS under constant current load

	Peukert number		Capacity (A h) at 1C	
	New	After 50 cycles	New	After 50 cycles
Battery alone	1.23	1.35	60	48.8
EDLC alone	1.05	1.05	0.45	0.45
Battery + EDLC	1.19	1.24	61.2	54.7

3.2 Change of Peukert number

Due to the EDLC have shared a large part of the current in transient operation, the battery unit in HPS is able to deliver more capacity than the battery stand alone due to Peukert phenomenon [11, 12]. Table 5 lists the Peukert numbers and the measured capacities of a solo battery and the HPS, at the first cycle and after 50 cycles, respectively. Peukert phenomenon is an empirical formula which approximates the variation of available capacity of a battery versus discharge rate as expressed in Eq. 5.

$$C_{\mathrm{p}} = I_{\mathrm{dis}}^{k} t_{\mathrm{dis}}. \tag{5}$$

where C_{p} is the theoretical capacity of the battery in A h, I_{dis} is the discharge current, t_{dis} is discharge time, and k is the Peukert constant. This equation shows that higher discharge current yields less available capacity in the battery. Generally, the Peukert constant indicates how well a battery performs under continuous discharge current and it usually varies from 1 to 1.3. In some extreme conditions, however, such as ultrahigh rate discharge or low temperature, the current–time relation does not follow the Peukert rule, and shows more nonlinear characteristics. In this circumstance, the Peukert number that may larger than 1.3 is no longer have its original meaning, but it is still an indicator of the battery performance. A value which is close to 1 indicates that the battery performs well; the higher the value is, the more the capacity loses when the battery is discharged at high current rate. As shown in Table 5, under −10 °C, the Peukert value of a new unit is reduced from 1.23 to 1.19 due to the EDLC. For the unit after 50 test cycles, this number decreases from 1.35 to 1.24.

3.3 Discharge capacity

The state of health is calculated based on the measured actual capacity at each cycle divided by the nominal capacity indicated by the manufacturer. The discharge capacity therefore is an important parameter that indicates the battery SoH.

Ambient temperature is a major influence on the battery capacity. Several studies [13, 14] have indicated that the lower the temperature, the fewer the capacity available. In pulse discharge applications, the degradation in capacity becomes more significant. Figure 12 depicts the capacity variations of the HPS and the battery in pulsed discharge test (10 s, 50 % duty cycle and under −10 °C) corresponding to the different cutoff voltage 10.8 and 10.0 V, respectively. It is indicated that the EDLC can increase the total capacity of the HPS in pulse discharge processes for both 10.8 and 10.0 V conditions, especially at high current rate. Allowing for the capacity of the EDLC is so small compared to the battery's (about 1.16 %), it is reasonable to consider that the battery capacity will be increased because the assistance of the supercap. The increased capacity ratio is defined by Eq. 6 and the values according to different current rate are shown in the right *Y*-axis of Fig. 12.

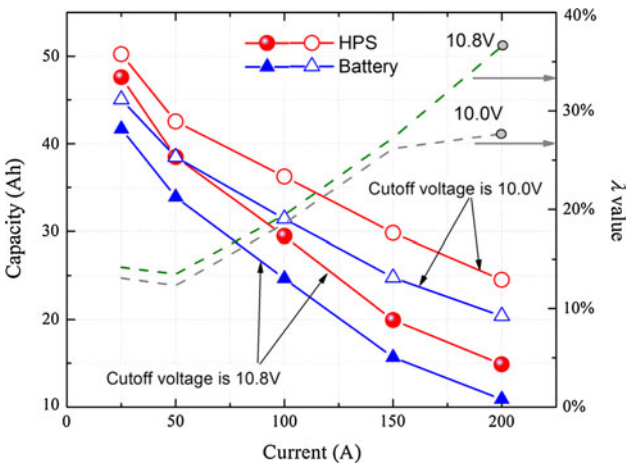

Fig. 12 Capacity variations under 10-s 50 % duty pulse discharge

$$\lambda = \frac{C_{\mathrm{HPS}}(I_{\mathrm{dis}}) - C_{\mathrm{Battery}}(I_{\mathrm{dis}})}{C_{\mathrm{Battery}}(I_{\mathrm{dis}})} \times 100\,\%, \tag{6}$$

where $C_{\mathrm{HPS}}(I_{\mathrm{dis}})$ and $C_{\mathrm{Battery}}(I_{\mathrm{dis}})$ are the discharge capacities of the HPS and the battery with respect to the current rate. For the 10.8 V voltage condition, as current rate increases from 25 to 200 A, λ increases from 14.2 to 36.6 %. While for the 10.0 V condition, λ varies from 13.1 to 27.7 %, substantially shows the same trend. Small difference between the two λ values at the point of Current = 200 A (points A and B in Fig. 12) may result from the following reason: the battery voltage drops more sharply at the final stage of discharge process (the shadowed area in Fig. 7), and the slope of voltage increases with discharge current. In 200 A discharge, the voltage drops so fast from 10.8 to 10 V, even with EDLC's assistance. Therefore, the contribution of the EDLC to the total capacity is not as significant as the effects shown in other current rates.

Figure 13 is a diagram illustrating the capacity increases of the HPS compared with the battery in the discharge

processes above. Under low temperature, the increase rates that correspond to all current values (red line in Fig. 13) are higher than the values measured under 25 °C. According to these results, one can recognize that, the EDLC plays a more significant role under low temperature.

The capacity variation with different pulse duration has also been studied (Fig. 14). It is indicated that, the smaller the duty cycle is, the larger the capacity will be. According to the discussion in Sect. 3.1, the current shared by the EDLC is determined by the resistance ratio and the time constant (Eq. 4). In a given pulse, the ESR ratio $R_b/(R_b + R_c)$ can be supposed to be invariable, and it is independent of the pulse time. While the current distribution varies with time: the current of EDLC/battery branch decreases/increases with the pulse duration, which means that the EDLC plays more significant role as the pulse duty cycle decreases (suppose that the period of pulse is fixed). In another words, the average battery current decreases with the pulse duty, in a series of pulse discharge processes with the same amplitude and period. Therefore, the capacity that the HPS can release in the short duty pulse is larger than that in the long duty pulse, according to the Peukert principle.

3.4 Performance in drive cycle

Although this article is mainly focused on the pulse discharge applications of the hybrid power system that is usually referred to a traditional cranking system, the HPS still has potential usage in other EV or HEV applications as main power supply. The most important issue in these applications is the power performance during acceleration and regenerative braking. Figure 15 illustrates the current distribution and characters of both the battery and the EDLC. During the first 200 s, the EDLC discharges more current than the battery. However, as discussed in Sect. 3.1, the EDLC component cannot sustain a large rate discharge because its terminal voltage is limited by the battery in this parallel topology. In the rest 1,200 s, the EDLC absorbs a large portion of current from the regenerative braking, while releases a small part of current compared with the lead-acid battery in discharge processes. This trend is indicated in Fig. 16: after the first 200 s, the discharge capacity of the EDLC stays around a certain level (about 0.033 A h) with small-scope fluctuations. This is consistent with the analysis above: the EDLC's voltage is limited by the battery and it varies in a relatively smaller range, so it cannot respond to high rate pulse demands (as EDLC only) due to its discharge/charge ability is linearly correlated with its voltage. To improve the EDLC performance as a peak power unit, the voltage of EDLC stack

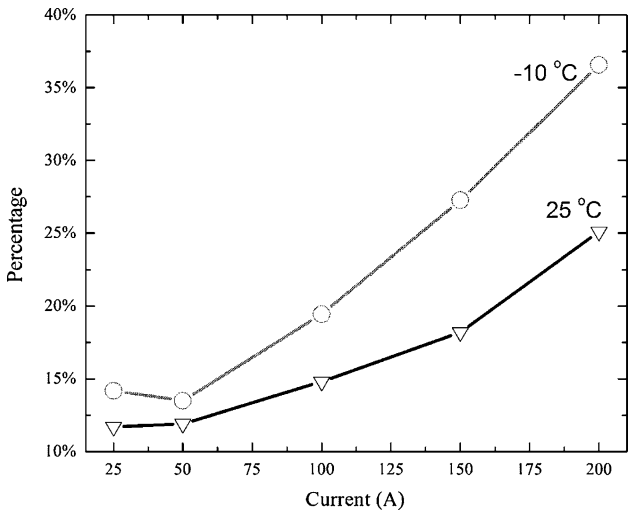

Fig. 13 Capacity increase rate of HPS to the battery standalone

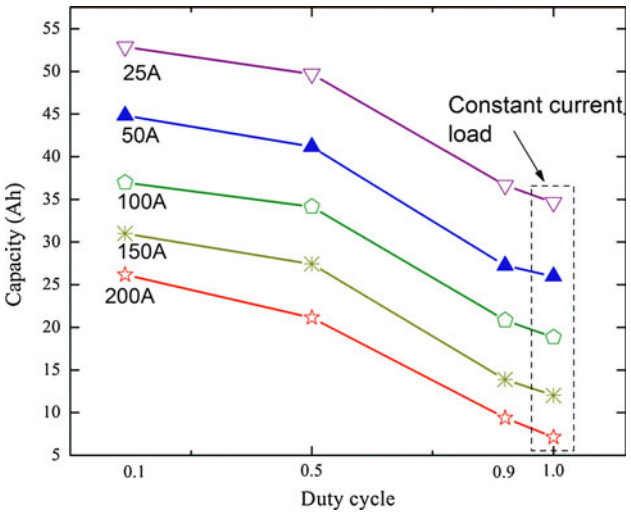

Fig. 14 The capacities under different current rates and duty cycles

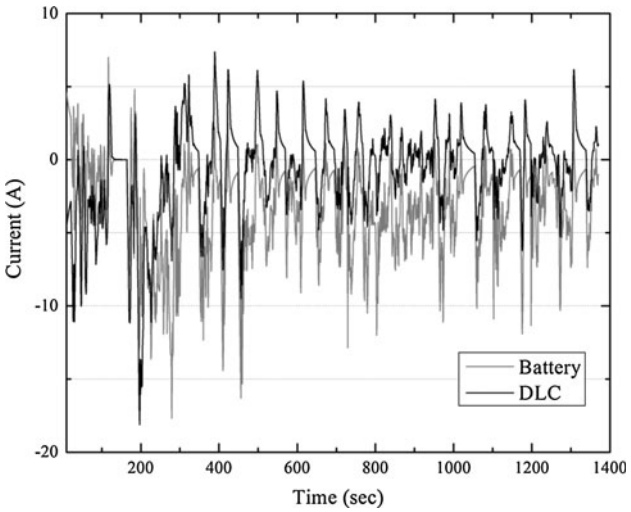

Fig. 15 Current distribution in UDDS test

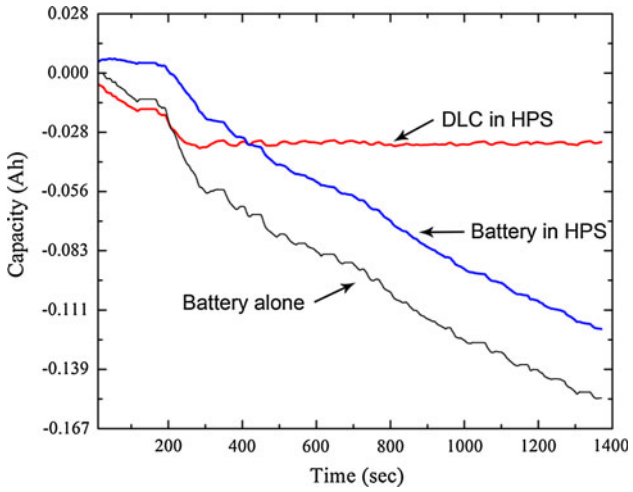

Fig. 16 A h discharged of one HPS unit in UDDS drive cycle

should be independent with the battery. Normally an EDLC voltage ranges from 50 to 100 % of its nominal voltage to keep an acceptable efficiency of the energy transfer [15]. A possible approach which will optimally use the EDLC's capacitance is adding a DC–DC converter between the EDLC and the battery, since the EDLC's terminal voltage will be decoupled from the battery's. The EDLC thus can yields better performance in absorbing the transient current. Taking the cost and the added complexity into account, however, there are still some difficulties in integrating a DC–DC converter in each HPS unit. For instance, modern EV propulsion system usually needs high bus voltage (280–380 V) to provide desired dynamic performance. Suppose that the PPS consists of 12 V HPS units in series, the required number of converters is about 24–32, which will significantly increase the overall cost and the complexity of the energy storage system. Consequently, at least in the current stage, designers still prefer the topology of a single DC–DC between the battery pack and the EDLC pack when constructing the EV's propulsion systems as mentioned in Sect. 1.

4 Conclusion

A systematic analysis of the performance of a hardwired parallel combination of the lead-acid battery and the EDLC is presented in this article. Under low temperature, pairing the EDLC with a lead-acid battery will prominently enhance the battery performance in high rate discharge applications, which could be the routine works of a vehicle cranking system in cold countries. An equivalent circuit model has been proposed to explain the current distribution and evolution of the components of the HPS, the calculated results fit well with the experimental values.

Under pulse current discharge tests operated at −10 °C, the energy available from a lead-acid battery increases as the pulse duty decreases. The increases in available capacity, compared to the capacity measured at constant current rate, amounted to 72, 58, and 4 % at 0.1, 0.5, and 0.9 duty cycle, respectively (calculated by 50 A discharge). These increments are larger than the values reported in former researches [13], which obtained mainly based on room temperature experiments.

While, applying this type of HPS (direct parallel connect) to the EV as main power source is not a sensible choice, because under continuous current load (regardless of constant or pulsed discharge processes), the EDLC only gives marginal contributions to the capacity since its voltage is limited by the parallel connected battery unit.

References

1. Kötz R, Carlen M (2000) Electrochim Acta 45:2483
2. Carter R, Cruden A (2008) In: International Symposium on Power Electronics, Electrical Drives, Automation and Motion, 2008. SPEEDAM 2008, p 727
3. Crolla DA, Ren Q, Eldemerdash S et al. (2008) In: IEEE Vehicle Power and Propulsion Conference 2008, VPPC '08, p 1
4. Onar O, Khaligh A (2008) In: IEEE Vehicle Power and Propulsion Conference 2008, VPPC '08, p 1
5. Holland CE, Weidner JW, Dougal RA et al (2002) J Power Sources 109:32
6. Smith TA, Mars JP, Turner GA (2002) In: The 33rd Annual IEEE Power Electronics Specialist Conference, p 124
7. Bode H (1977) Lead-acid batteries. Wiley, New York
8. Flores R, Blanco LM (1999) J Power Sources 78:30
9. Omar N, Van Mierlo J, Verbrugge B et al (2010) Electrochim Acta 55:7524
10. Bentley P, Stone DA, Schofield N (2005) J Power Sources 147:288
11. Caumont O, Le Moigne P, Rombaut C et al (2000) IEEE Trans Energy Convers 15:354
12. Peukert W (1897) Elektrotechnische Zeitschrift 27:287
13. Catherino HA, Burgel JF, Shi PL et al (2006) J Power Sources 162:965
14. Pascoe PE, Anbuky AH (2002) J Power Sources 111:304
15. Cooper A, Moseley PT (2003) J Power Sources 113:200